APCOM'07 in conjunction with EPMESC XI, *December 3-6, 2007, Kyoto, JAPAN*

Revisit of two classical elasticity problems by using the null-field BIE

Y. T. Lee, J. T. Chen*, K. S. Chou

Department of Harbor and River Engineering, National Taiwan Ocean University, 2 Pei-Ning Road, Keelung, 202-24, Taiwan

e-mail: D93520002@mail.ntou.edu.tw, *jtchen@mail.ntou.edu.tw, M95520083@mail.ntou.edu.tw

Abstract In this paper, the two classical elasticity problems, Lamé problem and stress concentration factor, are revisited by using the null-field integral equation. The null-field integral formulation is utilized in conjunction with degenerate kernel and Fourier series. To fully utilize the circular geometry, the fundamental solutions and the boundary densities are expanded by using degenerate kernels and Fourier series, respectively. In the two classical problems of elasticity, the null-field BIE is employed to derive the exact solutions.The Kelvin solution is first separated to degenerate kernel in this paper. After employing the null-field BIE, not only the stress but also the displacement field are obtained. In a similar way, Lamé problem is solved without any difficulty.

Key words: elasticity, degenerate kernel, Fourier series, null-field integral equation, SCF, Lamé problem

1. INTRODUCTION

Engineering problems always are simulated by using the mathematical models of boundary value problem, e.g., the steady state heat conduction problem [1], electrostatic potential [2] and torsion bar problems [3] are simulated by the Laplace equation; membrane vibration [4], acoustics [5] and water wave problems [6] are governed by the Helmholtz equation; plate vibration [7] and Stokes' flow [8] are formulated by the biharmonic equation. In order to solve the boundary value problems, researchers and engineers have paid more attention on the development of boundary integral equation method (BIEM), boundary element method (BEM) and meshless method than domain type methods, finite element method (FEM) and finite difference method (FDM). Among various numerical methods, BEM is one of the most popular numerical approaches for solving boundary value problems. Although BEM has been involved as an alternative numerical method for solving engineering problems, some critical issues exist, e.g. singular and hypersingular integrals, boundary-layer effect, ill-posed system and mesh generation.

Unlike the conventional BEM and BIEM, Waterman [9] introduced first the so-called T-matrix method for electromagnetic scattering problems. Various names, null-field approach or extended boundary condition method (EBCM), have been coined. The null-field approach or T-matrix method was used widely for obtaining numerical solutions of acoustics [10], elastodynamics [11] and hydrodynamics [12]. Boström [13] introduced a new method of treating the scattering of transient fields by a bounded obstacle in the three-dimensional space. He defined new sets of time-dependent basis functions, and use of these to expand the free space Green's function and the incoming and scattered fields. The method is a generalization to the time domain of the null-field approach first given by Waterman [9]. A crucial advantage of the null-field approach or T-matrix method consists in the fact that the influence matrix can be computed easily. Although many works for acoustic, elastodynamic and hydrodynamic problems have been done, only a few articles on elastostatics can be found [14]. The idea of changing the singularity distribution from real boundary to fictitious boundary (fictitious BEM) or putting the observation point outside the domain (null-field approach) can remove the singular and hypersingular integrals. However, they may result in an ill-posed matrix.

In the Fredholm integral equations, the degenerate kernel (or so-called separate kernel) plays an important role. However, its applications in practical problems seem to have taken a back seat to other methods. This degenerate kernel can be seen as one kind of approximation for fundamental solution, i.e., the kernel function is expressed as finite sums of products by two linearly independent functions. The concept of generating "optimal" degenerate kernels has been proposed by Sloan et al. [15]. They also proved it to be equivalent to the iterated Petrov-Galerkin approximation. Later, Kress [16] proved that the integral equations of the second kind in conjunction with degenerate kernels have the convergence rate of exponential order instead of the linear algebraic order of conventional BEM. Recently, Chen et. al. have applied null-field integral equation in conjunction with degenerate kernel and Fourier series to solve Laplace [17], Helmholtz [18], biharmonic [19] and biHelmholtz [20] problems with circular holes. They claimed five advantages, (1) free of calculating principal values, (2) exponential convergence, (3) elimination of boundary-layer effect, (4) meshless, and (5) well-posed system, using the null-field approach. Following the successes, we extended this approach to deal with inclusion problems [21]. In the approach, the principal value is avoided and the collocating on the real boundary using the null-field formulation achieved. We also found the rate of convergence of their approach is in the exponential order. Although we used the concept of null-field integral equation, we can locate the observer point exactly on the boundary free of facing singularity due to the introduction of degenerate kernels.

In this paper, we develope a systematic approach to deal with elasticity problems with circular boundaries. The null-field integral formulation is utilized in conjunction with degenerate kernel and Fourier series. To fully utilize the circular geometry, the fundamental solutions and the boundary densities are expanded by using degenerate kernels and Fourier series, respectively. This approach is seen as a semi-analytical method, since the error stems from the truncation of Fourier series in the implementation. The advantages, free of calculating principal value, meshless and well-posed system are expected. For the circular and annular problems, the analytical solution can be obtained by using the present method. Finally, the two classical problems, one is an infinite plate with a circular hole subject to remote tension (stress concentration factor problem) and another is an annular cylinder subject to uniform pressures (Lamé problem), were given to see the validity of the present approach.

2. METHODS OF SOLUTION

2.1 Problem statements

The two classical problems in the Timoshenko and Goodier's book [25] are revisted. One is an infinite plate with a circular hole subject to remote tension (stress concentration factor problem) and another is an annular cylinder subject to uniform pressures (Lamé problem) as shown in Figs. 1 and 2, respectively. The medium is considered as an isotropic, elastic and homogenous body. The governing equation is

$$(\lambda + G)\nabla(\nabla \cdot \underset{\sim}{u}(x)) + G\nabla^2 \underset{\sim}{u}(x) = 0, \quad x \in D, \tag{1}$$

where $u(x)$ is the displacement, D is the domain of interest, ∇^2 is the Laplacian operator, and λ and G are the Lamé constants for the isotropic elasticity.

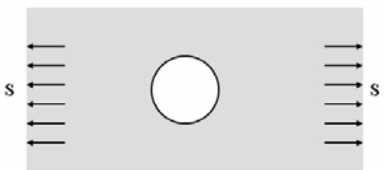

Fig. 1 An infinite plate with a circular hole subject to remote tesion

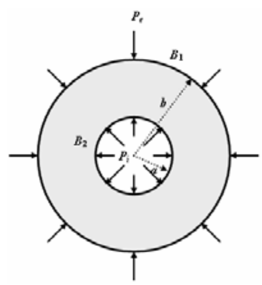

Fig. 2 An annular cylinder subject to uniform pressures

2.2 Dual null-field integral formulation

The direct formulation of boundary integral equation method stems from the reciprocal work theorem. We have the Somigliana's identity [22],

$$u_j(s) = \int_B U_{ij}(x,s) t_i(x)\, dB(x) - \int_B T_{ij}(x,s) u_i(x)\, dB(x), \quad s \in D, \tag{2}$$

$$0 = \int_B U_{ij}(x,s) t_i(x)\, dB(x) - \int_B T_{ij}(x,s) u_i(x)\, dB(x), \quad s \in D^c, \tag{3}$$

where $U_{ij}(x,s)$ and $T_{ij}(x,s)$ are the Kelvin free-space Green's function of the *i*th direction respons for displacement and traction, respectively, due to a concentrated load in the *j*th direction at the point s, and D^c denotes the complementary domain. Equations (2) and (3) can be changed to

$$u_i(x) = \int_B U_{ki}(s,x) t_k(s)\, dB(s) - \int_B T_{ki}(s,x) u_k(s)\, dB(s), \quad x \in D, \tag{4}$$

$$0 = \int_B U_{ki}(s,x) t_k(s)\, dB(s) - \int_B T_{ki}(s,x) u_k(s)\, dB(s), \quad x \in D^c. \tag{5}$$

The explicit form of $U_{ki}(s,x)$, or so-called Kelvin solution, is

$$U_{ki}(s,x) = \frac{-1}{8\pi G(1-\nu)} \left((3-4\nu)\delta_{ki} \ln(r) - \frac{y_i y_k}{r^2} \right), \tag{6}$$

where ν is the Poisson ratio, $y_i = s_i - x_i$ and $i = 1,2$ and $k = 1,2$ for the plane elasticity. Now, in order to obtain an additional independent equation, we apply the traction operator [23] to Eqs.(4) and (5).Then, we have

$$t_p(x) = \int_B L_{kp}(s,x) t_k(s)\, dB(s) - \int_B M_{kp}(s,x) u_k(s)\, dB(s), \quad x \in D, \tag{7}$$

$$0 = \int_B L_{kp}(s,x) t_k(s)\, dB(s) - \int_B M_{kp}(s,x) u_k(s)\, dB(s), \quad x \in D^c. \tag{8}$$

Equations (4) and (7) are coined the dual boundary integral equations for the domain point and Eqs.(5) and (8) are called the dual null-field integral equations. When the field point x is collocated on the real boundary, the dual boundary integral equations for the boundary point ($x \in B$) can be obtained as follows:

$$c_{ij} u_j(x) = R.P.V. \int_B U_{ki}(s,x) t_k(s)\, dB(s) - C.P.V. \int_B T_{ki}(s,x) u_k(s)\, dB(s), \quad x \in B, \tag{9}$$

where *R.P.V.* is the Riemann principal value, *C.P.V.* is the Cauchy principal value, and c_{ij} is equal to $\delta_{ij} - \mathcal{B}_{ij}$ in which $\mathcal{B}_{ij}$ depends on the solid angle and on the configuration of the corner at x of the boundary and on the Poisson ratio of the material of the body. At a smooth boundary, $\mathcal{B}_{ij}$ reduces to $\delta_{ij}/2$. By applying the traction operator to Eq.(9), we have

$$c_{pj} t_j(x) = C.P.V. \int_B L_{kp}(s,x) t_k(s)\, dB(s) - H.P.V. \int_B M_{kp}(s,x) u_k(s)\, dB(s), \quad x \in B, \tag{10}$$

where *H.P.V.* denotes the Hadamard principal value. A detailed discussion for the dual boundary integral equations can be found in the original article by Hong and Chen [23] and a review article of Chen and Hong [24]. It is noted that the conventional null-field integral equations are not singular since s and x never coincide. If the kernel functions in Eqs. (4), (5), (7) and (8) are substituted by using the appropriate degenerate (separable) kernels, we have

$$u_i(x) = \int_B U_{ki}(s,x) t_k(s)\, dB(s) - \int_B T_{ki}(s,x) u_k(s)\, dB(s), \quad x \in D \cup B, \tag{11}$$

$$t_p(x) = \int_B L_{kp}(s,x) t_k(s)\, dB(s) - \int_B M_{kp}(s,x) u_k(s)\, dB(s), \quad x \in D \cup B, \tag{12}$$

$$0 = \int_B U_{ki}(s,x) t_k(s)\, dB(s) - \int_B T_{ki}(s,x) u_k(s)\, dB(s), \quad x \in D^c \cup B, \tag{13}$$

$$0 = \int_B L_{kp}(s,x) t_k(s)\, dB(s) - \int_B M_{kp}(s,x) u_k(s)\, dB(s), \quad x \cup D^c \cup B. \tag{14}$$

It is found that the integral equations for the domain point or for the null-field point can include the collocation point on the real boundary since the appropriate degenerate kernels are used as elaborated on later.

2.3 Expansions of the fundamental solution and boundary density

To fully utilize the property of circular geometry, the mathematical tools, separable kernel (or so-called degenerate kernel) and Fourier series, are utilized for an analytical study.

2.3.1 Degenerate (separable) kernel for the fundamental solution

In order to derive the degenerate kernel, the polar coordinate is utilized to substitute the Cartesian coordinate. Therefore, the source and collocation points are expressed as (R,θ) and (ρ,ϕ), respectively, in the polar coordinate. The position vector of source point is $z_s = s_1 + s_2 i = Re^{i\theta}$. Similarly, the collocation point is $z_x = x_1 + x_2 i = \rho e^{i\phi}$. The former term ($\ln r$) in the bracket of Eq.(6) is the fundamental solution of Laplace equation and the degenerate kernel can be found in [17].

In order to expand the term ($\frac{y_i y_k}{r^2}$) in Eq.(6) into separable form, we have

$$\frac{1}{z_x - z_s} = \frac{1}{(\rho\cos\phi - i\rho\sin\phi) - (R\cos\theta - iR\sin\theta)} = \frac{(\rho\cos\phi - R\cos\theta) - i(\rho\sin\phi - R\sin\theta)}{\rho^2 + R^2 - 2R\rho\cos(\theta-\phi)} = \frac{y_1 - iy_2}{r^2}. \tag{15}$$

For the exterior case($R<\rho$), Eq.(15) can be expanded as follows

$$\frac{1}{z_x - z_s} = \frac{1}{z_x}\frac{1}{1-(z_s/z_x)} = \frac{1}{z_x}\left[1 + \frac{z_s}{z_x} + \left(\frac{z_s}{z_x}\right)^2 + \left(\frac{z_s}{z_x}\right)^3 + \left(\frac{z_s}{z_x}\right)^4 + \cdots\cdots\right] = \frac{1}{\rho}e^{-i\phi}\left[\sum_{m=0}^{\infty}\left(\frac{R}{\rho}\right)^m e^{im(\theta-\phi)}\right]. \tag{16}$$

After comparing Eq.(15) with Eq.(16), we obtain

$$\begin{aligned} \frac{y_1}{r^2} &= \frac{(\rho\cos\phi - R\cos\theta)}{\rho^2 + R^2 - 2R\rho\cos(\theta-\phi)} = \frac{1}{\rho}\sum_{m=0}^{\infty}\left(\frac{R}{\rho}\right)^m \cos(m\theta - (m+1)\phi), \\ \frac{y_2}{r^2} &= \frac{(\rho\cos\phi - R\cos\theta)}{\rho^2 + R^2 - 2R\rho\cos(\theta-\phi)} = \frac{1}{\rho}\sum_{m=0}^{\infty}\left(\frac{R}{\rho}\right)^m \sin((m+1)\phi - m\theta). \end{aligned} \tag{17}$$

Then, we have

$$\begin{aligned} \frac{y_1^2}{r^2} = &\sum_{m=0}^{\infty}\frac{1}{2}\left(\frac{R}{\rho}\right)^m \cos m(\theta-\phi) + \sum_{m=0}^{\infty}\frac{1}{2}\left(\frac{R}{\rho}\right)^m \cos(m\theta-(m+2)\phi) \\ &-\sum_{m=0}^{\infty}\frac{1}{2}\left(\frac{R}{\rho}\right)^{m+1} \cos((m+1)(\theta-\phi)) - \sum_{m=0}^{\infty}\frac{1}{2}\left(\frac{R}{\rho}\right)^{m+1} \cos((m-1)\theta-(m+1)\phi) \end{aligned} \tag{18}$$

$$\begin{aligned} \frac{y_2^2}{r^2} = &\sum_{m=0}^{\infty}\frac{1}{2}\left(\frac{R}{\rho}\right)^m \cos m(\theta-\phi) - \sum_{m=0}^{\infty}\frac{1}{2}\left(\frac{R}{\rho}\right)^m \cos(m\theta-(m+2)\phi) \\ &-\sum_{m=0}^{\infty}\frac{1}{2}\left(\frac{R}{\rho}\right)^{m+1} \cos((m+1)(\theta-\phi)) + \sum_{m=0}^{\infty}\frac{1}{2}\left(\frac{R}{\rho}\right)^{m+1} \cos((m-1)\theta-(m+1)\phi) \end{aligned} \tag{19}$$

$$\begin{aligned} \frac{y_1 y_2}{r^2} = &\sum_{m=0}^{\infty}\frac{1}{2}\left(\frac{R}{\rho}\right)^m \sin m(\theta-\phi) + \sum_{m=0}^{\infty}\frac{1}{2}\left(\frac{R}{\rho}\right)^m \sin(m\theta-(m+2)\phi) \\ &-\sum_{m=0}^{\infty}\frac{1}{2}\left(\frac{R}{\rho}\right)^{m+1} \sin((m+1)(\theta-\phi)) + \sum_{m=0}^{\infty}\frac{1}{2}\left(\frac{R}{\rho}\right)^{m+1} \sin((m-1)\theta-(m+1)\phi) \end{aligned}. \tag{20}$$

Similarly, we can obtain the separable form of terms of $\frac{y_i y_k}{r^2}$ for the interior case ($R>\rho$) as shown below:

$$\begin{aligned} \frac{y_1^2}{r^2} = &\sum_{m=0}^{\infty}\frac{1}{2}\left(\frac{\rho}{R}\right)^m \cos m(\phi-\theta) + \sum_{m=0}^{\infty}\frac{1}{2}\left(\frac{\rho}{R}\right)^m \cos(m\phi-(m+2)\theta) \\ &-\sum_{m=0}^{\infty}\frac{1}{2}\left(\frac{\rho}{R}\right)^{m+1} \cos((m+1)(\phi-\theta)) - \sum_{m=0}^{\infty}\frac{1}{2}\left(\frac{\rho}{R}\right)^{m+1} \cos((m-1)\phi-(m+1)\theta) \end{aligned} \tag{21}$$

$$\begin{aligned} \frac{y_2^2}{r^2} = &\sum_{m=0}^{\infty}\frac{1}{2}\left(\frac{\rho}{R}\right)^m \cos m(\phi-\theta) - \sum_{m=0}^{\infty}\frac{1}{2}\left(\frac{\rho}{R}\right)^m \cos(m\phi-(m+2)\theta) \\ &-\sum_{m=0}^{\infty}\frac{1}{2}\left(\frac{\rho}{R}\right)^{m+1} \cos((m+1)(\phi-\theta)) + \sum_{m=0}^{\infty}\frac{1}{2}\left(\frac{\rho}{R}\right)^{m+1} \cos((m-1)\phi-(m+1)\theta) \end{aligned} \tag{22}$$

$$\frac{y_1 y_2}{r^2}=\sum_{m=0}^{\infty}\frac{1}{2}\left(\frac{\rho}{R}\right)^m \sin m(\phi-\theta)+\sum_{m=0}^{\infty}\frac{1}{2}\left(\frac{\rho}{R}\right)^m \sin(m\phi-(m+2)\theta)$$
$$-\sum_{m=0}^{\infty}\frac{1}{2}\left(\frac{\rho}{R}\right)^{m+1} \sin((m+1)(\phi-\theta))+\sum_{m=0}^{\infty}\frac{1}{2}\left(\frac{\rho}{R}\right)^{m+1} \sin((m-1)\phi-(m+1)\theta) . \quad (23)$$

According to Eqs. (18)-(20) and (21)-(23), the degenerate kernel for the fundamental solution $U_{ki}(s,x)$, is obtained as

$$U_{11}(s,x)=\begin{cases} U_{11}^I(R,\theta;\rho,\phi)=-\dfrac{1}{8\pi G(1-\nu)}\Bigg[(3-4\nu)\left(\ln R-\sum_{m=1}^{\infty}\dfrac{1}{m}(\dfrac{\rho}{R})^m\cos(m(\theta-\phi))\right) \\ \quad -\dfrac{1}{2}\left(1+\sum_{m=0}^{\infty}(\dfrac{\rho}{R})^m\cos((m+2)\theta-m\phi)-\sum_{m=0}^{\infty}(\dfrac{\rho}{R})^{m+1}\cos((m+1)\theta-(m-1)\phi)\right)\Bigg], \quad R>\rho, \\ U_{11}^E(R,\theta;\rho,\phi)=-\dfrac{1}{8\pi G(1-\nu)}\Bigg[(3-4\nu)\left(\ln \rho-\sum_{m=1}^{\infty}\dfrac{1}{m}(\dfrac{R}{\rho})^m\cos(m(\theta-\phi))\right) \\ \quad -\dfrac{1}{2}\left(1+\sum_{m=0}^{\infty}(\dfrac{R}{\rho})^m\cos(m\theta-(m+2)\phi)-\sum_{m=0}^{\infty}(\dfrac{R}{\rho})^{m+1}\cos((m-1)\theta-(m+1)\phi)\right)\Bigg], \quad R<\rho, \end{cases} \quad (24)$$

$$U_{12}(s,x)=U_{21}(s,x)=\begin{cases} U_{12}^I(R,\theta;\rho,\phi)=\dfrac{1}{16\pi G(1-\nu)}\left(\sum_{m=0}^{\infty}(\dfrac{\rho}{R})^m\sin((m+2)\theta-m\phi)-\sum_{m=0}^{\infty}(\dfrac{\rho}{R})^{m+1}\sin((m+1)\theta-(m-1)\phi)\right), \quad R>\rho, \\ U_{12}^E(R,\theta;\rho,\phi)=\dfrac{1}{16\pi G(1-\nu)}\left(\sum_{m=0}^{\infty}(\dfrac{R}{\rho})^m\sin((m+2)\phi-m\theta)-\sum_{m=0}^{\infty}(\dfrac{R}{\rho})^{m+1}\sin((m+1)\phi-(m-1)\theta)\right), \quad R<\rho, \end{cases} \quad (25)$$

$$U_{22}(s,x)=\begin{cases} U_{22}^I(R,\theta;\rho,\phi)=-\dfrac{1}{8\pi G(1-\nu)}\Bigg[(3-4\nu)\left(\ln R-\sum_{m=1}^{\infty}\dfrac{1}{m}(\dfrac{\rho}{R})^m\cos(m(\theta-\phi))\right) \\ \quad -\dfrac{1}{2}\left(1-\sum_{m=0}^{\infty}(\dfrac{\rho}{R})^m\cos((m+2)\theta-m\phi)+\sum_{m=0}^{\infty}(\dfrac{\rho}{R})^{m+1}\cos((m+1)\theta-(m-1)\phi)\right)\Bigg], \quad R>\rho, \\ U_{22}^E(R,\theta;\rho,\phi)=-\dfrac{1}{8\pi G(1-\nu)}\Bigg[(3-4\nu)\left(\ln \rho-\sum_{m=1}^{\infty}\dfrac{1}{m}(\dfrac{R}{\rho})^m\cos(m(\theta-\phi))\right) \\ \quad -\dfrac{1}{2}\left(1-\sum_{m=0}^{\infty}(\dfrac{R}{\rho})^m\cos(m\theta-(m+2)\phi)+\sum_{m=0}^{\infty}(\dfrac{R}{\rho})^{m+1}\cos((m-1)\theta-(m+1)\phi)\right)\Bigg], \quad R<\rho, \end{cases} \quad (26)$$

and the three kernels ($T_{ki}(s,x)$, $L_{ki}(s,x)$ and $M_{ki}(s,x)$) can be obtained according to their definitions by using the traction operator in [23]. To the authors' best knowledge, the degenerate kernel for elasticity was not found in the literature before.

2.3.2 Fourier series expansion for boundary densities

We apply the Fourier series expansion to approximate the boundary displacement u_k and traction t_k on the boundary,

$$u_k(s_j)=a_{0,k}^j+\sum_{n=1}^{\infty}a_{n,k}^j\cos n\theta_j+b_{n,k}^j\cos n\theta_j, \quad s_j\in B_j, \quad j=1,2$$
$$t_k(s_j)=p_{0,k}^j+\sum_{n=1}^{\infty}p_{n,k}^j\cos n\theta_j+q_{n,k}^j\cos n\theta_j, \quad s_j\in B_j, \quad j=1,2 \quad (27)$$

where $a_{n,k}^j$, $b_{n,k}^j$, $p_{n,k}^j$ and $q_{n,k}^j$ ($k=1,2$) are the Fourier coefficients and θ_j is the polar angle. In the real computation, only M number of terms is used for the Fourier series.

3. Illustrative examples

The first example for verifying our formulation is an infinite plate with a circular hole subject to remote tenser. Figure 1 shows an infinite plate with a circular hole subject to a uniform tension of magnitude S in the x direction. The radius of the hole is a. The problem can be decomposed into two parts by using the superposition technique as shown in Figures 3(a) and 3(b). One is an infinite plate subject to a uniform tension and another is an infinite plate with a hole. In the boundary of the hole, it needs to satisfy the boundary conditions of free traction, $t_1 = 0$ and $t_2 = 0$, for the superposing total

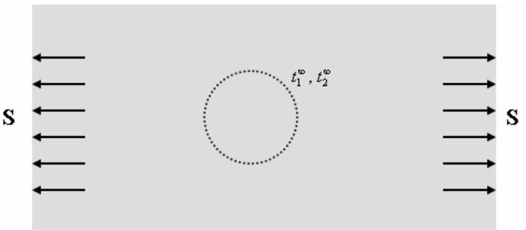

Fig. 3(a) An infinite plate subject to a uniform tension

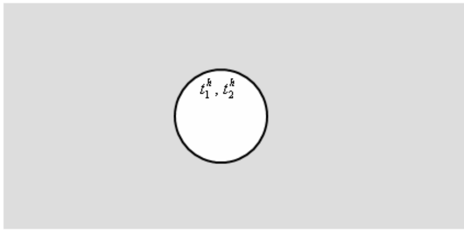

Fig. 3(b) An infinite plate with a hole

solution. According to the definition of traction, we obtain

$$t_1^\infty = \sigma_{11} \cdot n_1 + \sigma_{12} \cdot n_2 = -S\cos\theta, \quad t_2^\infty = \sigma_{21} \cdot n_1 + \sigma_{22} \cdot n_2 = 0, \tag{28}$$

From the boundary conditions of free traction, the traction on the circular boundary in Figure 3(b) is

$$t_1^h = S\cos\theta, \quad t_2^h = 0 \tag{29}$$

By using Eq.(24), we have

$$\begin{aligned} 0 = &\int_B U_{11}^I(s,x)\left(S\cos\theta\right)dB(s) - \int_B T_{11}^I(s,x)\left(a_{0,1}^h + \sum_{n=1}^{N} a_{n,1}^h \cos n\theta + \sum_{n=1}^{N} b_{n,1}^h \sin n\theta\right)dB(s) \\ &- \int_B T_{21}^I(s,x)\left(a_{0,2}^h + \sum_{n=1}^{N} a_{n,2}^h \cos n\theta + \sum_{n=1}^{N} b_{n,2}^h \sin n\theta\right)dB(s) \end{aligned}, \tag{30}$$

$$\begin{aligned} 0 = &\int_B U_{12}^I(s,x)\left(S\cos\theta\right)dB(s) - \int_B T_{12}^I(s,x)\left(a_{0,1}^h + \sum_{n=1}^{N} a_{n,1}^h \cos n\theta + \sum_{n=1}^{N} b_{n,1}^h \sin n\theta\right)dB(s) \\ &- \int_B T_{22}^I(s,x)\left(a_{0,2}^h + \sum_{n=1}^{N} a_{n,2}^h \cos n\theta + \sum_{n=1}^{N} b_{n,2}^h \sin n\theta\right)dB(s) \end{aligned}, \tag{31}$$

for the problem of an infinite plate with a hole in Figure 3(b). The kernels, $U_{11}^I(s,x)$, $U_{12}^I(s,x)$, $T_{11}^I(s,x)$, $T_{12}^I(s,x)$, $T_{21}^I(s,x)$ and $T_{22}^I(s,x)$ can be substituted by using the separable forms. Through the procedure of comparing the coefficients, we obtain

$$\begin{aligned} &a_{1,1}^h = \frac{(1-\nu)Sa}{G} \qquad a_{0,1}^h = a_{0,2}^h = a_{1,2}^h = a_{n,1}^h = a_{n,1}^h = 0 \quad (n = 2,3,\cdots) \\ &b_{1,2}^h = -\frac{(1-2\nu)Sa}{2G} \qquad b_{1,1}^h = b_{n,1}^h = b_{n,2}^h = 0 \quad (n = 2,3,\cdots) \end{aligned} \tag{32}$$

After determining the Fouries coefficients of boundary densities, the deformation fields are obtained by substituting the coefficients in Eq.(32) into Eq.(11). The representations of displacement fields are

$$\begin{aligned} u_1^h(x) &= \int_B U_{11}^E(s,x)\left(S\cos\theta\right)dB(s) - \int_B T_{11}^E(s,x)\left(\frac{(1-\nu)aS}{G}\cos\theta\right)dB(s) - \int_B T_{21}^E(s,x)\left(-\frac{(1-2\nu)aS}{2G}\sin\theta\right)dB(s) \\ u_2^h(x) &= \int_B U_{12}^E(s,x)\left(S\cos\theta\right)dB(s) - \int_B T_{12}^E(s,x)\left(\frac{(1-\nu)aS}{G}\cos\theta\right)dB(s) - \int_B T_{22}^E(s,x)\left(-\frac{(1-2\nu)aS}{2G}\sin\theta\right)dB(s) \end{aligned} \tag{33}$$

After substituting the degenerate kernels, the deformation fields are obtained as follows：

$$\begin{aligned} u_1^h(x) &= \frac{(1-\nu)S}{G}\frac{a^2}{\rho}\cos\phi + \frac{S}{4G}\frac{a^2}{\rho}\left(1 - \frac{a^2}{\rho^2}\right)\cos 3\phi \\ u_2^h(x) &= -\frac{(1-2\nu)S}{2G}\frac{a^2}{\rho}\sin\phi + \frac{S}{4G}\frac{a^2}{\rho}\left(1 - \frac{a^2}{\rho^2}\right)\sin 3\phi \end{aligned} \tag{34}$$

For another part solution in Figure 3(a), it is simulated by using a circular plate with the radius b. When the radius b approaches infinity, it is seen as an infinite plate. Based on this concept, we obtain the Fourier coefficients as shown beloow：

$$
\begin{aligned}
&a_{0,1}^{\infty} = a_{0,2}^{\infty} = arbitrary \\
&b_{1,1}^{\infty} = -a_{1,2}^{\infty} \\
&a_{1,1}^{\infty} = \frac{(1-\nu)Sb}{G}, \quad a_{n,1}^{\infty} = a_{n,2}^{\infty} = 0 \quad (n = 2,3,\cdots) \\
&b_{1,2}^{\infty} = -\frac{\nu Sb}{2G}, \quad b_{n,1}^{\infty} = b_{n,2}^{\infty} = 0 \quad (n = 2,3,\cdots)
\end{aligned} \tag{35}
$$

After determining the Fouries coefficients of boundary densities, the deformation fields are obtained by substituting the coefficients in Eq.(35) into Eq.(11).The coefficients, $a_{0,1}^{\infty}$, and $a_{0,2}^{\infty}$ are the rigid-body terms, and to ezros for simplicity. The representations of deformation fields are

$$
\begin{aligned}
u_1^{\infty}(x) &= \frac{(1-\nu)S\rho}{2G}\cos\phi + b_{1,1}^{\infty}\frac{\rho}{b}\sin\phi \\
u_2^{\infty}(x) &= -\frac{\nu S\rho}{2G}\sin\phi - b_{1,1}^{\infty}\frac{\rho}{b}\cos\phi
\end{aligned} \tag{36}
$$

Although there is a free coefficient ($b_{1,1}^{\infty}$), it can be neglected for the near field since the outer radius b is infinity. After determining the deformation fields for an infinite plate subject to a uniform tension and an infinite plate with a hole, the total deformation fields are

$$
\begin{aligned}
u_1 &= \frac{(1-\nu)S}{G}\frac{a^2}{\rho}\cos\phi + \frac{S}{4G}\frac{a^2}{\rho}\left(1-\frac{a^2}{\rho^2}\right)\cos 3\phi + \frac{(1-\nu)S\rho}{2G}\cos\phi \\
u_2 &= -\frac{(1-2\nu)S}{2G}\frac{a^2}{\rho}\sin\phi + \frac{S}{4G}\frac{a^2}{\rho}\left(1-\frac{a^2}{\rho^2}\right)\sin 3\phi - \frac{\nu S\rho}{2G}\sin\phi
\end{aligned} \tag{37}
$$

Based on the displacement fields, the stresses are easily obtained as

$$\sigma_{11} = \frac{[2\rho^4 - 3a^2\rho^2\cos 2\phi + a^2(3a^2 - 2\rho^2)\cos 4\phi]S}{\rho^4} \tag{38}$$

$$\sigma_{22} = \frac{[\rho^2\cos 2\phi + (3a^2 - 2\rho^2)\cos 4\phi]a^2 S}{2\rho^4} \tag{39}$$

$$\sigma_{12} = \frac{[-\rho^2 + (6a^2 - 4\rho^2)\cos 2\phi]a^2 S}{2\rho^4}\sin 2\phi \tag{40}$$

By using the tensor transformation [25], the stresses in the polar coordinate can be represented as

$$\sigma_{rr} = \frac{(\rho^2 - a^2)[\rho^2 + (\rho^2 - 3a^2)\cos 2\phi]S}{2\rho^4} \tag{41}$$

$$\sigma_{\theta\theta} = \frac{[\rho^2(\rho^2 + a^2) - (\rho^4 + 3a^4)\cos 2\phi]S}{2\rho^4} \tag{42}$$

$$\sigma_{r\theta} = \frac{(\rho^4 + 2a^2\rho^2 - 3a^4)S}{2\rho^4}\sin 2\phi \tag{43}$$

When $\rho = a$, Eqs. (41)-(43) are reduced to

$$\sigma_{rr} = \sigma_{r\theta} = 0 \tag{44}$$

$$\sigma_{\theta\theta} = S - 2S\cos 2\phi \tag{45}$$

The hoop stress distribution in Eq.(45) is the same as that of Timoshenko and Goodier's book [25]. When $\phi = \pi/2$ or $\phi = 3\pi/2$, the hoop stress ($\sigma_{\theta\theta}$) reaches the maximum of $3S$. However, it is not found for the displacement fields in the Timoshenko and Goodier's book [25]. Only Airy stress function and stress were obtained in their book. If we would like to know the displacement fields, it is necessary to calculate the strain through the Hooke's law. Then, the displacement fields can be determined from stress by integrating the strain. This procedure may be not straightforward and is time-consuming. In the proposed approach, not only the stress but also the displacement fields can be obtained directly at the same time. In Figure 4(a), it is obvious to observe that the plate is elongated uniformly in the x-axis direction since a uniform tension is given. The parameters of the material are given as $G=1$ and $\nu=0.3$. The deformation in Figure 4(b) occurs due to the boundary traction. Figure 4(c) shows the sketch of total deformation. Here, the magnitude S of the tension is 1, and the radius of the hole is 1. It can be found that the circular hole is distorted. The same result can be obtained by using the *LM* hypersingular formulation of Eq.(14) as well as using the *UT* singular formation of Eq.(13). Two alternatives are provided in the proposed formulation.

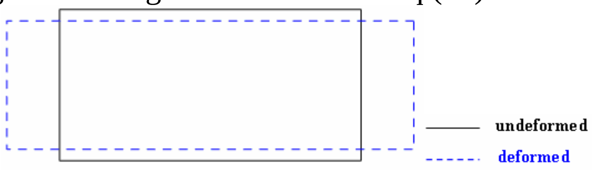

Fig. 4(a) Deformation of an infinite plate subject to a uniform tension

+

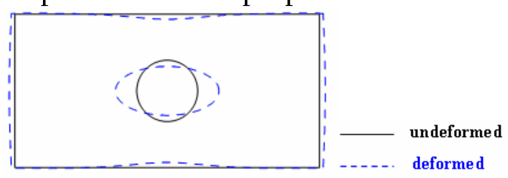

Fig. 4(b) Deformation of an infinite plate with a hole

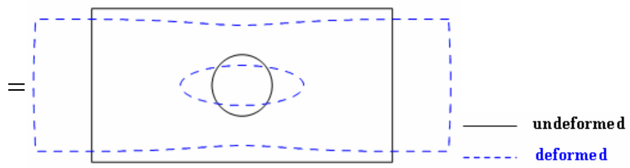

Fig. 4(c) Deformation of an infinite plate with a circular hole subject to remote tension

The second expamle is an annular cylinder subject to uniform pressures (the Lamé problem). In this example, the problem subject to uniform pressures on the inner and outer surfaces are considered. Let a and b denote the inner and outer radii of the annular cylinder where P_i and P_e are the uniform internal and external pressures as shown in Figure 2. Then the boundary conditions are shown below：

$$(\sigma_{rr})_{r=a}=-P_i \text{ and } (\sigma_{rr})_{r=b}=-P_e \tag{46}$$

This problem was first solved by Lamé [26]. Therefore, it is also called the Lamé problem. According to the definition of the traction, the boundary conditions of tractions are

$$t_1=\sigma_{11}\cdot n_1+\sigma_{12}\cdot n_2=-P_e\cos\theta,\quad t_2=\sigma_{21}\cdot n_1+\sigma_{22}\cdot n_2=-P_e\sin\theta \tag{47}$$

on the outer boundary B_1 and

$$t_1=\sigma_{11}\cdot n_1+\sigma_{12}\cdot n_2=P_i\cos\theta,\quad t_2=\sigma_{21}\cdot n_2+\sigma_{22}\cdot n_2=P_i\sin\theta \tag{48}$$

on the inner boundary B_2. The unknown boundary densities of displacement can be represented by using the Fourier series

$$u_1=a_0+\sum_{n=1}^{N}a_n\cos n\theta+\sum_{n=1}^{N}b_n\sin n\theta,\quad u_2=\overline{a}_0+\sum_{n=1}^{N}\overline{a}_n\cos n\theta+\sum_{n=1}^{N}\overline{b}_n\sin n\theta,\quad on\ B_1, \tag{49}$$

$$u_1=c_0+\sum_{n=1}^{N}c_n\cos n\theta+\sum_{n=1}^{N}d_n\sin n\theta,\quad u_2=\overline{c}_0+\sum_{n=1}^{N}\overline{c}_n\cos n\theta+\sum_{n=1}^{N}\overline{d}_n\sin n\theta,\quad on\ B_2. \tag{50}$$

By similarly using the null-field integral equation and Fourier series in Eq.(13), we obtain the Fourier coefficients as shown below：

$$\begin{aligned}
&a_0=c_0=arbitrary\\
&\overline{a}_0=\overline{c}_0=arbitrary\\
&b_1=d_1=-\overline{a}_1=-\overline{c}_1=arbitrary\\
&a_1=\overline{b}_1=\frac{b[(a^2+b^2(1-2\nu))P_e-2a^2(1-\nu)P_i]}{2(a^2-b^2)G}\\
&c_1=\overline{d}_1=\frac{a[2b^2(1-\nu)P_e-(b^2+a^2(1-2\nu))P_i]}{2(a^2-b^2)G}\\
&a_n=\overline{a}_n=b_n=\overline{b}_n=c_n=\overline{c}_n=d_n=\overline{d}_n=0\quad(n=2,3,\cdots)
\end{aligned} \tag{51}$$

After determining Fourier coefficients in Eq.(51), the deformation fields of Eq.(11) yield

$$u_1(\rho,\phi)=\frac{-(1-2\nu)P_e\rho}{4G(1-\nu)}\cos\phi+\frac{(1-2\nu)P_i}{4G(1-\nu)}\frac{a^2}{\rho}\cos\phi+a_1\frac{(1-2\nu)}{2(1-\nu)}\frac{\rho}{b}\cos\phi+c_1\frac{1}{2(1-\nu)}\frac{a}{\rho}\cos\phi+b_1\frac{\rho}{b}\sin\phi+a_0, \tag{52}$$

$$u_2(\rho,\phi)=\frac{-(1-2\nu)P_e\rho}{4G(1-\nu)}\sin\phi+\frac{(1-2\nu)P_i}{4G(1-\nu)}\frac{a^2}{\rho}\sin\phi+a_1\frac{(1-2\nu)}{2(1-\nu)}\frac{\rho}{b}\sin\phi+c_1\frac{1}{2(1-\nu)}\frac{a}{\rho}\sin\phi-b_1\frac{\rho}{b}\cos\phi+\bar{a}_0. \tag{53}$$

In Eqs. (52) and (53), the coefficients (a_1 and c_1) are found in Eq.(51) and b_1 and $\bar{a}_0$ are arbitrary values. The three terms ($b_1\frac{\rho}{b}\cos\phi$, a_0 and $\bar{a}_0$) can be seen as rigid body terms. The stresses are obtained as shown below

$$\sigma_{rr}(\rho)=\frac{a^2b^2(P_0-P_i)+(a^2P_i-b^2P_0)\rho^2}{(b^2-a^2)\rho^2} \tag{54}$$

$$\sigma_{\theta\theta}(\rho)=\frac{a^2b^2(P_i-P_0)+(a^2P_i-b^2P_0)\rho^2}{(b^2-a^2)\rho^2} \tag{55}$$

$$\sigma_{r\theta}(\rho)=0 \tag{56}$$

For the special case of zero outer pressure $P_e=0$, Eqs (54) and (55) are reduced to

$$\sigma_{rr}(\rho)=\frac{a^2P_i}{(b^2-a^2)}\left(1-\frac{b^2}{\rho^2}\right),\quad \sigma_{\theta\theta}(\rho)=\frac{a^2P_i}{(b^2-a^2)}\left(1+\frac{b^2}{\rho^2}\right) \tag{57}$$

These stress distributions are the same as Timoshenko and Goodier's solution [25]. As mentioned similarly in the Eample 1, only Airy stress function is found in their book. For the proposed approach, the displacement fields and stress can be obtained at the same time. The inner and outer radii are given 1 and 5, respectively. The uniform pressures are set as $P_e=1$ and $P_i=2$. The sketch of the deformation is shown in Fig. 5. Also, another alternative of the *LM* hypersingular formulation of Eq.(14) can be utilized to obtain the same result in the proposed approach.

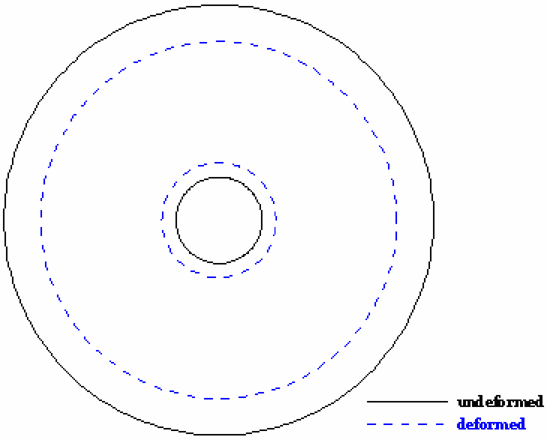

Fig. 5 Deformation of an annular cylinder subject to uniform pressures

4. Concluding remarks

For the elasticity problems with circular boundaries, we have proposed an analytical method by using the null-field integral formulation in conjunction with degenerate kernels and Fourier series. The advantages, free of calculating principal value, meshless and well-posed system were addressed. Besides, displacement as well as stress responses were both obtained at the same time. For the circular and annular cases, the analytical solutions were obtained by using the present method. Two illustrative examples, the stress concentration factor problem and the Lamé problem were demonstrated to see the validity of the analytical formulation. Good agreements were made after comparing the results with those of Timoshenko and Goodier's textbook.

References

[1] M. R. Barone and D. A. Caulk, *Optimal arrangement of holes in a two-dimensional heat conductor by a special boundary integral method*, Int. J. Numer. Meth. Engng., 18, (1982), 675-685.

[2] H. W. Cheng and L. Greengard, *On the numerical evaluation of electrostatic field in dense random dispersions of cylinders*, J. Comput. Phy., 136, 629-639.
[3] D. A. Caulk, *Analysis of elastic torsion in a bar with circular holes by a special boundary integral method*, ASME J. Appl. Mech., 50, (1983), 101-108.
[4] J. R. Hutchinson, *An alternative BEM formulation applied to membrane vibrations. Boundary Elements VII* (Eds. C. A. Brebbia and G. Maier), Berlin: Springer (1985).
[5] J. T. Chen and K. H. Chen, *Dual integral formulation for determining the acoustic modes of a two-dimensional cavity with a degenerate boundary*, Engng. Anal. Bound. Elem., 21(2), (1998), 105-116.
[6] K. H. Chen, J. T. Chen, C. R. Chou and C. Y. Yueh, *Dual boundary element analysis of oblique incident wave passing a thin submerged breakwater*. Engng. Anal. Bound. Elem., 26, (2002), 917-928.
[7] J. R. Hutchinson, *Vibration of plates, Boundary X* (Ed. C. A. Brebbia), Berlin: Springer (1988).
[8] R. D. Mills, *Computing internal viscous flow problems for the circle by integral methods*, J. Fluid Mech., 73, (1977), 609-624.
[9] P. C. Waterman, *Matrix formulation of electromagnetic scattering*, Proceedings of the IEEE, 53, (1965), 805-812.
[10] R. H. T. Bates, *Modal expansions for electromagnetic scattering from perfectly conducting cylinders of arbitrary cross-section*, Proceedings of the Institution of Electrical Engineers, 115, (1968), 1443-1445.
[11] P. C. Waterman, *Matrix theory of elastic wave scattering*, J. Acou.Soci. Amer., 60, (1976), 567-580.
[12] P. A. Martin, *On the null-field equations for water-wave radiation problems*, J. Fluid Mech, 113, (1981), 315-332.
[13] A. Boström, *Time-dependent scattering by a bounded obstacle in three dimensions*, J. Math. Phy., 23, (1982), 1444-1450.
[14] P. Olsson, *Elastostatics as a limit of elastodynamics – a matrix formulation*, Appl. Sci. Res., 41, (1984), 125-151.
[15] H. Kisu and T. Kawahara, *Boundary element analysis system based on a formulation with relative quantity*, *Boundary Elements X*, Brebbia CA, eds., Springer-Verlag, 1, (1988), pp. 111-121.
[16] J. T. Chen and H.-K. Hong, *Dual boundary integral equations at a corner using contour approach around singularity*, Adv. Engng. Soft., 21, (1994), 169-178.
[17] J. T. Chen, W. C. Shen and A. C. Wu, *Null-field integral equations for stress field around circular holes under anti-plane shear*. Engng. Anal. Bound. Elem., 30, (2005), 205-217.
[18] C. T. Chen, C. T. Chen, P. Y. Chen and I. L. Chen, *A semi-analytical approach for radiation and scattering problems with circular boundaries.*, Comp. Meth. Appl. Mech. Engng., 196, (2007), 2751-2764.
[19] J. T. Chen, C. C. Hsiao and S. Y. Leu, *Null-field integral equation approach for plate problems with circular boundaries*, ASME J. Appl. Mech., 73, (2006), 679-693.
[20] W. M. Lee, J. T. Chen and Y. T. Lee, *Free vibration analysis of circular plates with multiple circular holes using indirect BIEMs*, J. Sound Vib., 304, (2007), 811–830.
[21] J. T. Chen and A. C. Wu, *Null-field approach for the multi-inclusion problem under anti-plane shears*, ASME J. Appl. Mech., 74, (2007), 469-487.
[22] P. K. Banerjee and R. Butterfield, *Boundary element method in engineering science*. McGraw-Hill, New York, (1981).
[23] H.-K. Hong and J. T. Chen, *Derivations of Integral Equations of Elasticity*, J. Engng. Mech., ASCE, 114(6), (1988), 1028-1044.
[24] J. T. Chen and H.-K. Hong, *Review of dual boundary element methods with emphasis on hypersingular integrals and divergent series*. ASME Appl. Mech. Rev., 52,(1999),17-33.
[25] S. P. Timoshenko and J. N. Goodier, *Theory of elasticity*, New York: McGraw-Hill, (1970).
[26] G. Lamé, *Leçons sur la théorie de l'élasticité*, Gauthier-Villars, Paris, (1852).